JOURNAL OF COMPUTATIONAL PHYSICS 2, 154-177 (1967)

A Detached Shock Calculation by Second-Order Finite Differences[1]

ARNOLD LAPIDUS

Courant Institute of Mathematical Sciences, New York University, New York, New York 10012

ABSTRACT

A detached shock problem for a symmetric curved convex cylindrical body moving parallel to its plane of symmetry was solved by using a third-order accurate Richtmyer form of the Lax-Wendroff conservation equations. One innovation is an easy to use "artificial viscosity" term which preserves the high order of accuracy of the calculation while removing the nonlinear instabilities which otherwise appear in the shock region and near boundaries. Another innovation is a simple transformation of Cartesian space which changes the curved body into a straight line, thus reducing the large number of special points and irregularly shaped mesh regions which would otherwise appear in the difference method calculation. Such transformations are shown to preserve the conservation property of the system of differential equations. Other aspects of the third-order artificial viscosity term and the transformation are discussed. The results of a numerical calculation on a CDC 6600 computer are compared with known results.

I. INTRODUCTION

Consider a smooth plane-symmetric convex cylindrical body moving parallel to its axis of symmetry with constant supersonic speed through a perfect compressible gas. A steady state consists of a detached shock at some distance from the body which has a shape that depends on the shape of the body and its speed. There is a region of flow behind the shock and in front of the body in which the flow is subsonic, and a region behind the shock in which the flow is supersonic, these regions being separated by the so-called sonic line. The problem which is considered here is to determine the position of the shock near the sonic region and the flow in the sonic region for a specific case in which the steady-state configuration looks like Fig. 1.

[1] The work presented in this paper was supported by the AEC Computing and Applied Mathematics Center, Courant Institute of Mathematical Sciences, New York University, under Contract AT(30-1)—1480 with the U.S. Atomic Energy Commission.

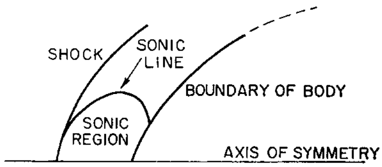

FIG. 1. Steady state configuration.

In Burstein's work [5] a time-dependent flow which tends to the steady state is calculated with conservation equations, and the shock is determined as a region of rapid variation of the flow quantities; we proceed similarly. The new features here compared with [5] are:

(1) A simpler artificial viscosity term is used.

(2) Since the boundary of the body is a curve instead of a straight line, a transformation of the Cartesian plane is effected which maps the curved body onto a straight vertical line, and the finite difference calculation is carried out in this nonphysical coordinate system. The conservation laws are rewritten as conservation laws in this new system.

(3) To continue calculating near the upper boundary of the mesh, flow quantities are extrapolated from the interior points to the boundary.

Finite difference methods of third-order accuracy similar to those in [5] were employed in the computation except near the body and the artificial upper boundary where the methods used were only second order to keep the computation from becoming unstable. The stability and accuracy of the computation will be discussed in the following sections on the differential equations and in later sections on the numerical results.

II. Differential Equations

Fundamental in this approach to solving the detached shock problem is the use of the conservation form [2, 3] of the equations of time-dependent, two-dimensional compressible fluid dynamics:

$$\frac{\partial U}{\partial t} + \frac{\partial F(U)}{\partial x} + \frac{\partial G(U)}{\partial y} = 0, \tag{1}$$

where

$$U = \begin{bmatrix} \rho \\ m \\ n \\ e \end{bmatrix} \qquad F(U) = \begin{bmatrix} m \\ m^2/\rho + p \\ mn/\rho \\ (e+p)\, m/\rho \end{bmatrix} \qquad G(U) = \begin{bmatrix} n \\ mn/\rho \\ n^2/\rho + p \\ (e+p)\, n/\rho \end{bmatrix},$$

in which

- x, y are cartesian coordinates
- t is time
- ρ is mass per unit volume
- u is the horizontal velocity component
- v is the vertical velocity component
- m is $\rho \cdot u$
- n is $\rho \cdot v$
- e is total energy per unit volume
- p is given by $e = p/(\gamma - 1) + \rho(u^2 + v^2)/2$, and
- γ is the ratio of specific heats (we are assuming a gamma-law gas).

In this approach the shock is not a boundary but simply an interior region of rapid variation of the flow quantities. In fact the reason for using the conservation form of the equations is that it includes the shock conditions as well as the differential equations of motion of the gas. Later we will use a transformation of space.

The following theorem shows that if a nonsingular transformation of space is made, then any conservation law expressed in the old coordinates can always be rewritten as a conservation law in the new coordinates.

THEOREM 1. *Under nonsingular space transformations, conservation laws are transformed into conservation laws.*

Proof: A conservation law is expressed by

$$\int_G U_t \, dx + \int_{\partial G} F_n \, dS = 0, \tag{2}$$

where $F_n = (\mathbf{F}, \mathbf{n})$, in which $\mathbf{F}$ is a vector $(F_1, ..., F_m)$ and $\mathbf{n} = (n_1, ..., n_m)$ is the normal to the surface G.

After a change invariables from $x_1, ..., x_m$ to $\xi_1, ..., \xi_m$ we want to show that (2) changes into an equation of the same form in the new coordinates. Let

$$J = \partial(x_1, ..., x_m)/\partial(\xi_1, ..., \xi_m),$$

and let J_s be the Jacobian for the surface element of (2). Let M be a matrix which transforms the direction of the normal ν to the surface in $(\xi_1, ..., \xi_m)$ space into the direction $\mathbf{n}$ of the associated normal to the surface in $(x_1, ..., x_m)$ space. The integral (2) becomes

$$\int_{\bar{G}} (\bar{U}J)_t \, d\xi + \int_{\partial\bar{G}} (\bar{F} \cdot \mathbf{n}) J_s \, d\bar{S} = 0, \tag{3}$$

where overbars denote the quantities in the new coordinate system. Now

$$(\bar{F} \cdot \mathbf{n}) \, J_s = (J_s \cdot \bar{F}, \mathbf{n}) = (J_s\bar{F}, M \cdot \nu) = (M^T J_s \bar{F}, \nu),$$

where M^T means transpose of M. This shows that $(\bar{F} \cdot \mathbf{n}) \, J_s$ is the component of a vector normal to $\bar{S}$ and therefore (2) and (3) are of the same form. Q.E.D.

A practical way to determine the components of the flux is given by the following. Use the differential form (1) of the conservation laws. By using the chain rule and multiplying (1) by J we get

$$(J\bar{U})_t + \left(\sum_{j=1}^{m} \sum_{k=1}^{m} \frac{\partial \bar{F}_j}{\partial \xi_k} \frac{\partial \xi_k}{\partial x_j} \right) J = 0. \tag{3a}$$

According to the theorem, the spatial part of (3a) is in conservation form; it is not hard to show that it is

$$(J\bar{U})_t + \sum_{k=1}^{m} \left(\sum_{j=1}^{m} J\bar{F}_j \frac{\partial \xi_k}{\partial x_j} \right)_{\xi_k} = 0. \tag{3b}$$

It is amusing that the validity of (3b) follows from the conceptual argument presented. Of course, (3b) can also be verified by a computation. We note that (3a) can be written as

$$(J\bar{U})_t + \sum_{j=1}^{m} \frac{\partial(x_1, ..., x_{j-1}, \bar{F}_j, x_{j+1}, ..., x_m)}{\partial(\xi_1, ..., \xi_m)}.$$

But according to a theorem of advanced calculus

$$\frac{\partial(x_1, ..., x_{j-1}, \bar{F}_j, x_{j+1}, ..., x_n)}{\partial(\xi_1, ..., \xi_n)}$$

is of the form $\sum (p_k)_{\xi_k}$ [11].

Specifically, the transformation which we used was

$$\xi_1 = x/h(y) \qquad \xi_2 = y, \tag{4}$$

in which $h'(y)$ exist and $h(y) \neq 0$. This changes the fundamental Eq. (1) into

$$[h(\xi_2)U]_t + [f - h'(\xi_2) \cdot \xi_1 g_1]_{\xi_1} + (gh)_{\xi_2} = 0, \tag{5}$$

and maps the curve $x = h(y)$ into the line $\xi_1 = 1$. In this problem the curve $x = h(y)$ is the boundary of the body.

Such a transformation of the space of independent variables is employed as a means of simplifying computation near the body. It is obvious from Theorem 1 [Eq. (3b)] that the transformation does not affect the existence of the shock or its position.

In summary, we have shown that the conservation properties of the system are preserved under the transformation and that the essential properties of the shock are also preserved under the transformation. It is also obvious that if the function h satisfies the symmetry property $h(y) = h(-y)$, then the symmetry of the solution to the transformed system is also preserved.

III. Geometry

The exterior of the obstacle in which the flow takes place is unbounded. Since only a finite number of lattice points can be employed in any actual computation, the neighborhood of infinity has to be dealt with in some summary fashion. In this work, we resort to the simple and crude expedient of confining the calculation to a finite region of the flow field which contains the whole sonic regime.

In this approach the region is bounded from above by an artificial boundary line on which boundary conditions have to be imposed which approximate well the state of affairs along this line in the true solution. At any rate, the error incurred by imposing artificial boundary conditions should be comparable to discretization errors.

The remaining geometrical inconvenience is the incommensurability of a curved body with a rectangular mesh. We solved that problem by mapping the irregularly shaped cut-out configuration onto a rectangular region by a transformation which took the boundary of the body into the right side of a rectangle. The mapping which we used was

$$\xi_1 = x/h(y) \qquad \xi_2 = y,$$

where $x = h(y)$ is the function which traces out the boundary of the body and is assumed to be continuously differentiable, symmetric in y, and nonvanishing. Then the Jacobian of the transformation is also nonvanishing.

Choose the coordinates so that the left boundary of Fig. 2 is the line $x = 0$; then its image is the line $\xi_1 = 0$. The lines $y = 0$ and $y = .2$ are transformed into $\xi_2 = 0$ and $\xi_2 = .2$, while the curve $x = h(y)$ is transformed into the line $\xi_1 = 1$. Figure 3 illustrates the new configuration in which the three previously straight boundaries remain so while the curved body is transformed into a line.

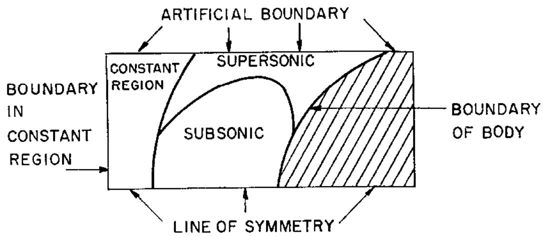

FIG. 2. Finite region containing subsonic region.

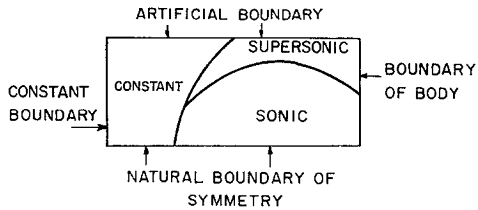

FIG. 3. The finite region after transformation.

This transformation also saves some computer space because the region behind the body, the shaded space in Fig. 2, has been eliminated.

The mesh which was chosen for the machine computation is a 79×20 rectangular grid projected onto that rectangular portion of $\xi_1\xi_2$ space given by $[0, 1] \times [0, y_{\max}]$. It is the set of points $(j\Delta\xi_1, k\Delta\xi_2)$ with $j = 0,..., 78; k = 0,..., 19$; and $\Delta\xi_1 = 1/78$, $\Delta\xi_2 = y_{\max}/19$. The body is denoted by the right-sided boundary of the mesh since the boundary of the body is transformed into the line $\xi_1 = 1$. The shock is not introduced as an explicit boundary but is determined as the locus of the most rapid change in the values of appropriate flow quantities.

In summary, a region of interest is cut from the plane and then transformed into a rectangle. The rectangular region is then represented as a rectangular mesh which can be used in a machine computation.

IV. DIFFERENCE EQUATIONS

In this Section, a difference scheme for the fundamental Eq. (1) which is similar to that in [2] is described and is shown to be consistent and to have truncation error $O(\Delta^3)$ in the smooth part of the flow which is far from shocks, body, or other boundaries. We hoped that no special methods would have to be used at the shock except to use the two-step scheme and that the location of the shock could be determined by sharp variations in some of the flow quantities such as density, entropy, or pressure. The main reason for this is that the two-step scheme is itself conservative as shown by Lax and Wendroff in [3]. That is, solutions U of the two-step equations satisfy a discrete analogue of the integral relation

$$\iiint [w_t U + w_x F(U) + w_y G(U)]\, dx\, dy\, dt = 0, \tag{6}$$

where $w(x, y, t)$ is a differentiable function of compact support. Such difference schemes are conjectured to satisfy the entropy condition. The *first step* of the two-step scheme is:

$$\begin{aligned} U^{n+\frac{1}{2}}_{j+\frac{1}{2},\,k+\frac{1}{2}} &= \frac{1}{4}(U^n_{jk} + U^n_{j+1\,k} + U^n_{jk+1} + U^n_{j+1\,k+1}) \\ &\quad - \frac{\Delta t}{2\Delta x}(F^n_{j+1\,k+\frac{1}{2}} - F^n_{j\,k+\frac{1}{2}}) - \frac{\Delta t}{2\Delta y}(G^n_{j+\frac{1}{2}\,k+1} - G^n_{j+\frac{1}{2}\,k}). \end{aligned} \tag{7a}$$

The *second step* of the scheme is:

$$U^{n+1}_{jk} = U^n_{jk} - \frac{\Delta t}{\Delta x}(\bar{F}^{n+\frac{1}{2}}_{j+\frac{1}{2}\,k} - \bar{F}^{n+\frac{1}{2}}_{j-\frac{1}{2}\,k}) - \frac{\Delta t}{\Delta y}(\bar{G}^{n+\frac{1}{2}}_{j\,k+\frac{1}{2}} - \bar{G}^{n+\frac{1}{2}}_{j\,k-\frac{1}{2}}), \tag{7b}$$

in which

$$U^n_{jk} = \begin{bmatrix} \rho^n_{jk} \\ m^n_{jk} \\ n^n_{jk} \\ e^n_{jk} \end{bmatrix}, F^n_{jk} = \begin{bmatrix} m^n_{jk} \\ (m^n_{jk})^2/\rho^n_{jk} + p^n_{jk} \\ m^n_{jk} \cdot n^n_{jk}/\rho^n_{jk} \\ (e^n_{jk} + p^n_{jk}) \cdot m^n_{jk}/\rho^n_{jk} \end{bmatrix}, G^n_{jk} = \begin{bmatrix} n^n_{jk} \\ m^n_{jk} \cdot n^n_{jk}/\rho^n_{jk} \\ (n^n_{jk})^2/\rho^n_{jk} + p^n_{jk} \\ (e^n_{jk} + p^n_{jk})\, n^n_{jk}/\rho^n_{jk} \end{bmatrix} \tag{7c}$$

and

$$\begin{aligned} \bar{F}^{n+\frac{1}{2}}_{j+\frac{1}{2}\,k} &= (F^{n+\frac{1}{2}}_{j+\frac{1}{2}\,k+\frac{1}{2}} + F^{n+\frac{1}{2}}_{j+\frac{1}{2}\,k-\frac{1}{2}})/2; \\ \bar{G}^{n+\frac{1}{2}}_{j\,k+\frac{1}{2}} &= (G^{n+\frac{1}{2}}_{j+\frac{1}{2}\,k+\frac{1}{2}} + G^{n+\frac{1}{2}}_{j-\frac{1}{2}\,k+\frac{1}{2}})/2. \end{aligned} \tag{7d}$$

This is a nine-point scheme in the sense that only nine points of the mesh at time $n \cdot \Delta t$ are needed to obtain numerical values at a point at time $(n + 1)\,\Delta t$. However, four additional points (A, B, C, D of Fig. 4) are used for the computation of intermediate values. This scheme can be used only for points which have all eight neighbors.

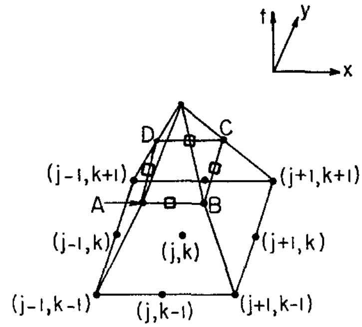

FIG. 4. The basic cell.

Next we want to prove consistency for this scheme [Eq. (7)] and also that the discretization error is $O(\Delta^3)$.

Let the *truncation error* at a point be defined as the difference between a computed solution and the true solution having the same initial data. This is also called *discretization error.*

THEOREM 2. *The scheme described by formula* (7) *is consistent with the fundamental Eq.* (1) *and has a truncation error which is* $O(\Delta^3)$ *in the smooth part of the flow.*

Proof. Define the operators $N(U)$ and $N_\Delta(U)$ by the equations

$$N(U) = U_t + F_x + G_y$$

and

$$N_\Delta(U) = (U_{jk}^{n+1} - U_{jk}^n)/\Delta t + (\bar{F}_{j+\frac{1}{2}\,k}^{n+\frac{1}{2}} - \bar{F}_{j-\frac{1}{2}\,k}^{n+\frac{1}{2}})/\Delta x + (\bar{G}_{j\,k+\frac{1}{2}}^{n+\frac{1}{2}} - \bar{G}_{j\,k-\frac{1}{2}}^{n+\frac{1}{2}})/\Delta y.$$

In order to prove the consistency of the operators N and N_Δ it will be shown that

$$\lim_{\Delta\to 0} | N^{n+\frac{1}{2}}(U) - N_\Delta^{n+\frac{1}{2}}(U)| = 0$$

for arbitrary smooth functions U. First we assume that

$$(\bar{F}_{j+\frac{1}{2}\,k}^{n+\frac{1}{2}} - \bar{F}_{j-\frac{1}{2}\,k}^{n+\frac{1}{2}})/\Delta x = F_x(U_{jk}^{n+\frac{1}{2}}) + O(\Delta) \tag{8a}$$

and

$$(\bar{G}_{j\,k+\frac{1}{2}}^{n+\frac{1}{2}} - \bar{G}_{j\,k-\frac{1}{2}}^{n+\frac{1}{2}})/\Delta y = G_y(U_{jk}^{n+\frac{1}{2}}) + O(\Delta), \tag{8b}$$

in which quantities on the left are evaluated by the difference scheme and the quantities on the right are evaluated by the assumed known function U. Then we have

$$| N^{n+\frac{1}{2}}U - N_{\Delta}^{n+\frac{1}{2}}U |$$

$$= \left| U_t^{n+\frac{1}{2}} + F_x^{n+\frac{1}{2}} + G_y^{n+\frac{1}{2}} - \frac{U_{jk}^{n+1} - U_{jk}^{n}}{\Delta t} - F_x^{n+\frac{1}{2}} - G_y^{n+\frac{1}{2}} + O(\Delta) \right|$$

$$= | U_t^{n+\frac{1}{2}} - U_t^{n+\frac{1}{2}} + O(\Delta)| = | O(\Delta)|$$

which goes to 0 as $\Delta \to 0$.

Now we still have to prove (8a) and (8b). The proof is complicated by the fact that the approximations to the derivatives in the difference scheme have an intermediate step. Only the proof of (8a) follows. The proof of (8b) would follow similar lines. To make the proof a little clearer, the function values which are computed from the difference scheme are denoted by V's. Then

$$\bar{F}_{j+\frac{1}{2}\,k}^{n+\frac{1}{2}} = [F(V_{j+\frac{1}{2}\,k+\frac{1}{2}}^{n+\frac{1}{2}}) + F(V_{j+\frac{1}{2}\,k-\frac{1}{2}}^{n+\frac{1}{2}})]/2 \tag{7d}$$

$$F(V_{j+\frac{1}{2}\,k+\frac{1}{2}}^{n+\frac{1}{2}}) = \bar{P}(U_{jk}^{n}, U_{j+1,\,k}^{n}, U_{j\,k+1}^{n}, U_{j+1\,k+1}^{n}), \tag{9}$$

where $\bar{P}$ is a very smooth function of U_{jk}^n, $U_{j+1\,k}^n, \ldots$. We are assuming that U is a smooth function of x, y, and t, so

$$F(V_{j+\frac{1}{2},\,k+\frac{1}{2}}^{n+\frac{1}{2}}) = P(\Delta x, \Delta y) \qquad \text{where } P \text{ is a smooth function of } \Delta x \text{ and } \Delta y \tag{10}$$

and

$$P(\Delta x, \Delta y) = P(0,0) + P_1(0,0)\,\Delta x + P_2(0,0)\,\Delta y + P_{11}(0,0)\frac{\Delta x^2}{2} + P_{12}(0,0)\,\Delta x\,\Delta y + P_{22}(0,0)\frac{\Delta y^2}{2} + O(\Delta^3). \tag{11}$$

Then by (7d) and (11) we obtain

$$\frac{\bar{F}_{j+\frac{1}{2}\,k}^{n+\frac{1}{2}} - \bar{F}_{j-\frac{1}{2}\,k}^{n+\frac{1}{2}}}{\Delta x} = \frac{F(V_{j+\frac{1}{2}\,k+\frac{1}{2}}^{n+\frac{1}{2}}) + F(V_{j+\frac{1}{2}\,k-\frac{1}{2}}^{n+\frac{1}{2}})}{2\Delta x} - \frac{F(V_{j-\frac{1}{2}\,k+\frac{1}{2}}^{n+\frac{1}{2}}) + F(V_{j-\frac{1}{2}\,k-\frac{1}{2}}^{n+\frac{1}{2}})}{2\Delta x} = 2P_1(0,0) + O(\Delta x^2). \tag{12}$$

Next, we will show that $2P_1(0, 0) = F_x(x, y, t) + O(\Delta t)$, which will finish the proof of consistency. From (9) and (7a) we obtain

$$P(\Delta x, \Delta y) = F\{(\tfrac{1}{4}[U(x,y,t) + U(x+\Delta x, y, t) + U(x, y+\Delta y, t) + U(x+\Delta x, y+\Delta y, t)] - (\Delta t/2\Delta x)[F(U(x+\Delta x, y, t)) - F(U(x,y,t))] - \Delta t/2\Delta y \cdot [G(U(x, y+\Delta y, t)) - G(U(x,y,t))]\}. \tag{13}$$

Then by differentiating (13) with respect to Δx we get

$$P_1(\Delta x, 0)$$
$$= F_U \cdot \{U_x/2 - \Delta t/2\Delta x \cdot (F_U U_x - [F(U(x + \Delta x, y, t)) - F(U(x, y, t))]/\Delta x)\}, \quad (14)$$

and for $\Delta x \to 0$

$$P_1(0, 0) = F_U \cdot [U_x/2 - F_{xx}\, \Delta t/4] = F_x(x, y, t)/2 + O(\Delta t).$$

This completes the proof of consistency.

Now we will show that the discretization error in the smooth part of the flow is $O(\Delta^3)$. Let the solution of the differential equation be $U(x, y, t)$ and let the result of calculating the approximation to the solution at time $t + \Delta t$ from values of the solution at time t be denoted by V_{jk}^{n+1}. We want to show

$$U(x, y, t + \Delta t) - V_{jk}^{n+1} = O(\Delta^3). \quad (15)$$

From the differential equation we find that

$$U(x, y, t + \Delta t)$$
$$= U(x, y, t) - \Delta t[F_x(x, y, t + \Delta t/2) + G_y(x, y, t + \Delta t/2)] + O(\Delta^3), \quad (16)$$

and from the difference scheme

$$V_{jk}^{n+1} = U(x, y, t) - \frac{\Delta t}{\Delta x}(\bar{F}^{n+\frac{1}{2}}_{j+\frac{1}{2}\,k} - \bar{F}^{n+\frac{1}{2}}_{j-\frac{1}{2}\,k}) - \frac{\Delta t}{\Delta y}(\bar{G}^{n+\frac{1}{2}}_{j\,k+\frac{1}{2}} - \bar{G}^{n+\frac{1}{2}}_{j\,k-\frac{1}{2}}), \quad (17)$$

where $\bar{F}$ and $\bar{G}$ are given by Eq. (7d). From (17) it is clear that Eq. (15) will be satisfied if

$$(\bar{F}^{n+\frac{1}{2}}_{j+\frac{1}{2}\,k} - \bar{F}^{n+\frac{1}{2}}_{j-\frac{1}{2}\,k})/\Delta x = F_x(x, y, t + \Delta t/2) + O(\Delta^2), \quad (18)$$

and similarly for the term in $G(V)$. To prove this, define $P(\Delta x, \Delta y)$ so that

$$F(V^{n+1}_{j+\frac{1}{2}\,k+\frac{1}{2}}) = P(\Delta x, \Delta y)$$
$$= F\left|\begin{array}{l} [U(x,y,t) + U(x+\Delta x,y,t) + U(x,y+\Delta y,t) + U(x+\Delta x,y+\Delta y,t)]/4 \\ -\dfrac{\Delta t}{2\Delta x}\left[\dfrac{F(x+\Delta x,y,t) + F(x+\Delta x,y+\Delta y,t)}{2} - \dfrac{F(x,y,t) + F(x,y+\Delta y,t)}{2}\right] \\ -\dfrac{\Delta t}{2\Delta y}\left[\dfrac{G(x,y+\Delta y,t) + G(x+\Delta x,y+\Delta y,t)}{2} - \dfrac{G(x,y,t) + G(x+\Delta x,y,t)}{2}\right] \end{array}\right|$$

(19)

From (19) it is clear that the equations

$$F(V^{n+\frac{1}{2}}_{j-\frac{1}{2}\,k+\frac{1}{2}}) = P(-\Delta x, \Delta y); \qquad F(V^{n+\frac{1}{2}}_{j+\frac{1}{2}\,k-\frac{1}{2}}) = P(\Delta x, -\Delta y);$$
$$F(V^{n+\frac{1}{2}}_{j-\frac{1}{2}\,k-\frac{1}{2}}) = P(-\Delta x, -\Delta y) \tag{20}$$

hold. If we assume that $U(x, y, t)$ is sufficiently smooth, we can expand P as

$$\begin{aligned} P(\Delta x, \Delta y) = {} & P(0, 0) + P_1(0, 0)\, \Delta x + P_2(0, 0)\, \Delta y \\ & + P_{11}(0, 0)\, \Delta x^2/2 + P_{12}(0, 0)\, \Delta x\, \Delta y \\ & + P_{22}(0, 0)\, \Delta y^2/2 + O(\Delta^3). \end{aligned} \tag{21}$$

From (20) and (21) it then follows that

$$\begin{aligned} & [F(V^{n+\frac{1}{2}}_{j+\frac{1}{2}\,k+\frac{1}{2}}) + F(V^{n+\frac{1}{2}}_{j+\frac{1}{2}\,k-\frac{1}{2}})/2\Delta x - F(V^{n+\frac{1}{2}}_{j-\frac{1}{2}\,k+\frac{1}{2}}) + F(V^{n+\frac{1}{2}}_{j-\frac{1}{2}\,k-\frac{1}{2}})/2\Delta x] \\ & \qquad = 2P_1(0, 0) + O(\Delta^2). \end{aligned} \tag{22}$$

We will now show that

$$P_1(0, 0) = F_x(x, y, t + \Delta t/2)/2 + O(\Delta^2), \tag{23}$$

and then (22) implies (18). That is, it is sufficient to show (23) in order to show that the discretization error is $O(\Delta^3)$.

To show (23), we differentiate (19) with respect to Δx and obtain

$$\begin{aligned} P_1(0, 0) = {} & \lim_{\substack{\Delta x \to 0 \\ \Delta y \to 0}} F_U[U(x, y, t) - \Delta t/2\, (F_x + G_y)] \\ & \cdot \left\{ U_x(x, y, t)/2 - \frac{\Delta t}{2\Delta x}\, [F_x(x + \Delta x, y, t)] \right. \\ & \left. + \frac{\Delta t}{2\Delta x} \left[\frac{F(x + \Delta x, y, t) - F(x, y, t)}{\Delta x} \right] - \frac{\Delta t}{2} \frac{G_{xy}}{2} \right\}. \end{aligned}$$

Then using the hypothesis that $U(x, y, t)$ is a solution to the fundamental equation, we get

$$\begin{aligned} P_1(0, 0) & = F_U[U(x, y, t + \Delta t/2)] \cdot \tfrac{1}{2}[U_x(x, y, t) + \Delta t/2 (U_t)_x] + O(\Delta^2) \\ & = F_U[U(x, y, t + \Delta t/2)]/2 \cdot U_x(x, y, t + \Delta t/2) + O(\Delta^2) \\ & = F_x(x, y, t + \Delta t/2)/2 + O(\Delta^2). \end{aligned}$$

Q.E.D.

We have now proved that this nine-point difference scheme is consistent with the fundamental Eq. (1) and has truncation error $O(\Delta^3)$ in the interior parts of the mesh which are not in the shock region. The left boundary has constant values and those at the axis of symmetry are computed by reflection. We still have to describe the difference schemes which are applied at the two nontrivial boundaries: the body and the upper artificial boundary.

At the upper boundary the flow quantities were evaluated by linear extrapolation as follows:

$$U_{jk}^{n+1} = 2U_{j-1\,k-1}^{n+1} - U_{j-2\,k-2}^{n+1}\,. \tag{24}$$

If the Mach cone at every point of the upper boundary were to leave the rectangular region of calculation, the errors introduced by extrapolation (24) would hopefully not affect the accuracy of the computation. While the Mach cones do not leave the region, the curves which are the envelopes of Mach cones starting at the artificial boundary end at points on the body which are still in the supersonic region. The numerical experiments show that errors which are introduced at the upper boundary affect the subsonic region only slightly. The linear extrapolation (24) is in a 45° degree direction which was roughly the same as that of the nearby characteristics. Scheme (24) was unstable at the early stages of calculation and therefore was replaced by (25), where the factor r was only gradually built up to 1.

$$U_{jk}^{n+1} = U_{j-1\,k-1}^{n+1} + r(U_{j-1\,k-1}^{n+1} - U_{j-2\,k-2}^{n+1}), \tag{25}$$

in which r has the following values according to the number of cycles:

r	No. cycles
.5	< 100 and > 0
.6	< 200 and > 99
.7	< 300 and > 199
.8	< 400 and > 299
.9	< 500 and > 399
1.0	$< \infty$ and > 499

The top point of the body is also treated in this *ad hoc* fashion of a point on the upper boundary, but the other points of the body are treated in a manner which is very much in the spirit of the conservation law approach. To explain the scheme used at the body we will refer to Fig. 5.

The flow quantities are assumed to be known at the points labelled 1, 2, 3, 4, 5, and 6 at time t. The problem is to obtain values of the flow quantities for the point labelled 1 at time $t + \Delta t$.

We think of the flow quantities at point 1 as being affected only by the fluxes F and G across the dotted lines. To obtain good estimates of F and G across those lines we first make estimates of the flow quantities at the points labelled 7, 8, 9, and 10 at time $t + \Delta t/2$.

At 7 (and 10) we calculate as at ordinary intermediate points. That is, for the point 7 we consider the rectangle whose vertices are the points 1, 4, 5, and 6. To

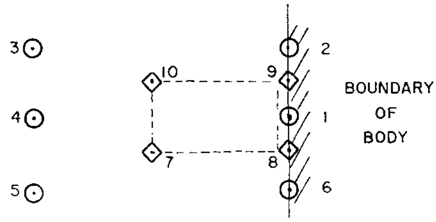

FIG. 5. Difference scheme at the body. ⊙, Mesh point; ◇, intermediate point.

compute the change in the flow quantities at point 7, we compute the sum of the fluxes through the sides of the rectangle and add it to the flow quantities. At time t, the average of the flow quantities at points 1, 4, 5, and 6 was used as an estimate for the values at point 7.

A point such as 8(or 9) has to be treated in a special way. The method chosen is to estimate its flow quantities at time t by averaging those at points 1 and 6. Since point 8 is in the same large rectangle (1, 4, 5, 6) as point 7, the change in the flow quantities due to fluxes is taken to be the same as at 7.

Having computed the flow quantities at time $t + \Delta t/2$ for the points 7, 8, 9, and 10, we use these values to compute the flux across the dotted lines to give the change in the value of the flow quantities at point 1 between time t and $t + \Delta t$. The formulas which follow express the various quantities involved in the procedure described above.

$$\begin{aligned}\text{Flux into rectangle } (1, 4, 5, 6) &= B_{78} \\ &= -\frac{\Delta t}{2\Delta x}\left[(F_6{}^n + F_1{}^n)/2 - (F_4{}^n + F_5{}^n)/2\right] \cdot T_1(y) \\ &\quad - \frac{\Delta t}{2\Delta x}\left[(G_6{}^n + G_1{}^n)/2 - (G_4{}^n + G_5{}^n)/2\right] \cdot T_2(x, y) \\ &\quad - \frac{\Delta t}{2\Delta y}\left[(G_1{}^n + G_4{}^n)/2 - (G_5{}^n + G_6{}^n)/2\right] \end{aligned} \tag{26a}$$

$$V_7^{n+\frac{1}{2}} = \frac{1}{4}(U_1{}^n + U_4{}^n + U_5{}^n + U_6{}^n) + B_{78}^{n+\frac{1}{2}} \tag{26b}$$

$$V_8^{n+\frac{1}{2}} = \frac{1}{2}(U_1{}^n + U_6{}^n) + B_{78}^{n+\frac{1}{2}}, \tag{26c}$$

where $T_1(y) = 1/h(y)$ $T_2(x, y) = -xh'(y)/h(y)$.

The same formulas with the appropriate changes in subscripts (referring to points in the figure) are used to obtain intermediate values at the points numbered 9 and 10. At the point numbered 1 the difference formula is:

$$U_1^{n+1} = U_1^n - \frac{2\Delta t}{\Delta x}\,[(F_9^{n+\frac{1}{2}} + F_8^{n+\frac{1}{2}})/2 - (F_7^{n+\frac{1}{2}} + F_{10}^{n+\frac{1}{2}})/2] \cdot T_1(y)$$
$$- T_2(x, y)\left(\frac{2\Delta t}{\Delta x}\right)[(G_9^{n+\frac{1}{2}} + G_8^{n+\frac{1}{2}})/2 - (G_7^{n+\frac{1}{2}} + G_{10}^{n+\frac{1}{2}})/2]$$
$$- \left(\frac{2\Delta t}{\Delta y}\right)[(G_9 + G_{10})/2 - (G_8 + G_7)/2]. \tag{27}$$

This difference scheme is consistent but has an error of second order rather than third order as at ordinary points.

The physical boundary condition is that the flow should be parallel to the wall at body points. This was not used so far; we impose it now by replacing the momentum vector calculated at boundary points by one which has the same magnitude and the right direction. Denoting by m' and n' the new momenta, we have

$$\omega = [(m^{n+1})^2 + (n^{n+1})^2]^{1/2}$$
$$\omega\eta \rightarrow m'^{\,n+1} \qquad -\omega\xi \rightarrow n'^{\,n+1}, \tag{28}$$

where (ξ, η) are the components of the normal to the body at the point.

At the nose of the body, the symmetry of the configuration is used to reduce the point to an ordinary point of the body. This is the same procedure used at other points of the axis of symmetry, i.e., the point is reduced to a known type by continuing the flow so that the point gets its full complement of neighbors.

We have now explained the difference method used in the mesh and at boundaries and also discussed the consistency and truncation error of the equations. The transformed equations were used in the conservation form as well as in the (analytically) equivalent form:

$$U_t + F_x \cdot h^{-1}(y) - x \cdot G_x \cdot h'(y) \cdot h^{-1}(y) + G_y = 0. \tag{29}$$

The results indicate that (5) gives much better accuracy for these equations than (29).

V. Stability: Simplified Lax-Wendroff Artificial Viscosity

The major difficulty in this problem was maintaining numerical stability. At various times instabilities appeared near the body, near the shock, and at the upper boundary. To counteract this instability we introduced a new type of stabilizing transformation which consisted of replacing the flow quantities U^{n+1} calculated in the last section by new ones, U'^{n+1}, obtained by smoothing first in the ξ_1 direction and then in the ξ_2 direction according to the following prescription.

$$U'^{n+1}_{jk} = U^{n+1}_{jk} + \lambda C \cdot \Delta'[| \Delta' u^{n+1}_{j+1\,k} | \cdot \Delta'(U^{n+1}_{j+1\,k})] \tag{30a}$$

$$U''^{n+1}_{jk} = U'^{n+1}_{jk} + \lambda C \cdot \Delta''[| \Delta'' v'^{n+1}_{j+1\,k} | \cdot \Delta''(U'^{n+1}_{j+1\,k})], \tag{30b}$$

where $\Delta' U_{jk} = U_{jk} - U_{j-1\,k}$; $\Delta'' U_{jk} = U_{jk} - U_{jk-1}$; and C is a constant (taken as 4 in actual computations) while u and v' are horizontal and vertical fluid velocity components.

Equations (30a, b) are fractional steps [8] for the numerical solution of the diffusion equation

$$U_t = \lambda C(\Delta^3)[(| u_{\xi_1} | U_{\xi_1})_{\xi_1} + (| v_{\xi_2} | U_{\xi_2})_{\xi_2}].$$

From this equation it is clear that smoothing is of third order and consequently does not affect the truncation error of the difference scheme.

Adding such a term to the equations of motion is similar to the von Neumann-Richtmyer approach used in [6] and was motivated by the higher order artificial viscosity of Lax and Wendroff [3].

In [3] Lax and Wendroff introduced a class of difference approximations to differential conservation laws which themselves are in discrete conservation form. We now describe this class and for the sake of simplicity we do it in only one space variable.

Let the differential conservation law be

$$U_t = F_x \qquad \text{where} \quad F = F(U),$$

with initial conditions $U(x, 0) = \phi(x)$. Let g be a function of 2ℓ arguments which has the property that

$$g(U,..., U) = F(U). \tag{31}$$

Consider the following difference approximation to the equation $U_t = F_x$:

$$\Delta v/\Delta t = \Delta g/\Delta x, \tag{32}$$

where

$$\Delta v = v(x, t + \Delta t) - v(x, t), \qquad v(x, 0) = \phi(x) \tag{33}$$

and

$$\Delta g = g(x + \Delta x/2) - g(x - \Delta x/2) \tag{34}$$

with

$$g(x + \Delta x/2) = g(v_{-\ell+1}, v_{-\ell+2}, \ldots, v_\ell), \tag{35}$$

where the v's are at points distributed symmetrically around $x + \Delta x/2$.

Multiply equation (32) by a smooth test vector of compact support, integrate with respect to x, and sum over all values of t which are integer multiples of Δt. On the left side apply summation by parts; on the right side replace the variables of integration by $x + \Delta x/2$ and $x - \Delta x/2$ in the two integrals which appear there. If $g(x)$ is defined at nonmesh points by linear interpolation from $g(x + \Delta x/2)$ and $g(x - \Delta x/2)$, we obtain

$$\begin{aligned} -\sum \int \frac{w(x,t) - w(x, t - \Delta t)}{\Delta t} v(x,t)\, dx\, \Delta t - \int w(x,0)\, \phi(x)\, dx \\ = -\sum \int \frac{w(x + \Delta x/2) - w(x - \Delta x/2)}{\Delta x} g(x)\, dx\, \Delta t. \end{aligned} \tag{36}$$

This leads to the following Lax-Wendroff theorem.

Consistency Theorem. *Let v be the solution of the difference equation* (32) *in conservation form with initial conditions ϕ and suppose that as Δt, $\Delta x \to 0$, v tends boundedly almost everywhere to some limit U. Then U is a solution of the differential conservation law and has initial values ϕ.*

This consistency theorem is actually central to the way that we are computing the shocked flow. We already know that solutions to the integral equation

$$\iint (w_t U - w_x F)\, dx\, dt + \int w(x,0)\, \phi(x)\, dx = 0 \tag{37}$$

satisfy the differential equations, the initial conditions, and the shock conditions. The consistency theorem says that solutions to (32) approximate the solutions to (37) near the shock as well as in the smooth region. Then, to compute shocked flows we merely have to iterate flow quantities by using an equation of the class defined by (32).

We show now that if we apply smoothing to solutions of difference equations in conservation form, the smoothed functions also satisfy difference equations in conservation form. More precisely:

Smoothing Theorem. *If a difference scheme satisfies a conservation law, and if smoothing is done by adding a term which is a first difference of a function S which has the two properties*

$$S = S(U_{-\ell}, U_{-\ell+1}, \ldots, U_{\ell-1})$$
$$S(U, U, \ldots, U) = 0,$$

then the scheme with smoothing also satisfies the same conservation law.

The proof follows simply by constructing

$$g_1(x - \Delta x/2) = g(U_{-\ell}, U_{-\ell+1}, ..., U_{\ell-1}) + S(U_{-\ell+1}, ..., U_\ell)$$

and using the difference scheme:

$$\frac{\Delta v}{\Delta t} = \frac{\Delta g_1}{\Delta x}.$$

It is clear from the definition of S that $g_1(U, U, ..., U) = F(U)$, which implies that the consistency theorem holds for g_1 as well as for g.

Such smoothing has been used by Kasahara [9] in atmospheric fluid dynamics problems and by Rusanov [10] in a variety of time-dependent problems. Kasahara reported that he used second-order smoothing once every forty cycles to maintain stability instead of third-order smoothing at each step as in this report. We tried a calculation in which we smoothed at alternate cycles. It became unstable very quickly.

In this section we have explained the reasons for using smoothing. We have shown that the smoothing retains all the accuracy that the original system had and that consistency in the sense of the integral operator is also preserved. In the next section the results of a machine computation at Mach 6 will be discussed.

VI. Computation

A. Test Case

The flow chosen for a test case was one computed by Eva Swenson and reported by her in [4]. This flow had plane symmetry and included a detached shock whose shape was prescribed to be

$$x = 3(1 + y^2)^{1/2},$$

where x is the distance along the axis of symmetry and y is the distance from the axis of symmetry. The gas was assumed to be perfect with gamma = 1.4. The Mach number at ∞ was 6. This inverse problem was solved to five figures of accuracy by Garabadian's method of characteristics in complex space [7], and furnished the body used in our calculation.[2]

B. Initial Flow

Our time-dependent method requires initial values of the flow quantities at interior points as well as at the body points. The choice of this initial flow is to

[2] Since the position of the body was not known at precisely the points needed by our finite difference method, we used quadratic interpolation to obtain the needed values.

a certain extent arbitrary. Presumably, the flow will eventually settle down to the correct steady state no matter what data one starts with. Of course, the closer our initial guess comes to representing the stationary flow, the faster it will converge to a steady state. In our calculation the initial data at the body were the results computed by Swenson; those at the upstream boundary were assigned the data at ∞. The initial flow quantities at all other points were arbitrarily set to be linear functions of ξ, and had the above data at the body and at the left boundary.

It was noticed that with initial data in which the pressure and density at the body were set equal to their values at ∞, the calculational scheme became unstable after a few cycles. A possible explanation for this instability is that these initial values are too far from the steady-state solution and initially give rise to too violent a flow. A way out of the difficulty was to iterate a number of cycles by using only the first step of the two-step method. This procedure is known to be stable. These numerical results indicate that if fluxes are too large, the two-step method is unstable. This is an instance of nonlinear instability, because for linear systems, stability is not influenced by the size of the initial data. At present, I know of no explanation for this instability nor for the subsequent stability of the scheme when applied to the more accurate data.

The usual stability analysis based on von Neumann criteria is not applicable here because in that theory one has to assume that flow quantities at neighboring lattice points differ by $O(h)$, whereas in our calculation this instability occurred in the shock region where the flow quantities vary rapidly.

C. Verifications

In this section we compare the results of our calculation with the exact steady state known from Swenson's work. We also present various flow quantities as functions of time.

1. *Bernoulli Steady-State Constant*

In [1, p. 300] it is proved that for a steady flow the quantity

$$B = (u^2 + v^2)/2 + 1/(\gamma - 1) \cdot C^2$$

is a constant along every streamline even when the streamline crosses a shock. Since each streamline comes from upstream, B is a constant throughout. The initial average of B is 29.04. The final average of B is 28.59. The correct upstream value is 28.700. The average of B as a function of cycle number is plotted in Fig. 6.

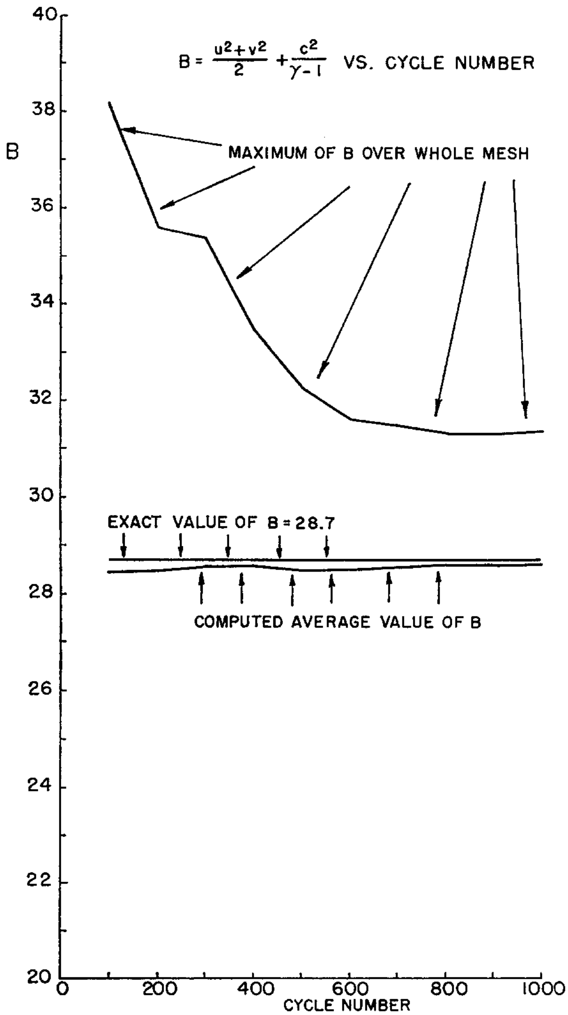

FIG. 6. Computed values of B vs cycle number.

2. *Stagnation Point Pressure*

Figure 7 illustrates the pressure at the stagnation point as a function of cycle number. The pressure at cycle number 0 is the steady-state theoretical pressure p^* consistent with the parameters of the problem. The graph shows that the pressure, which starts out at p^*, drops very rapidly, then turns around, overshoots p^*, and finally approaches it asymptotically.

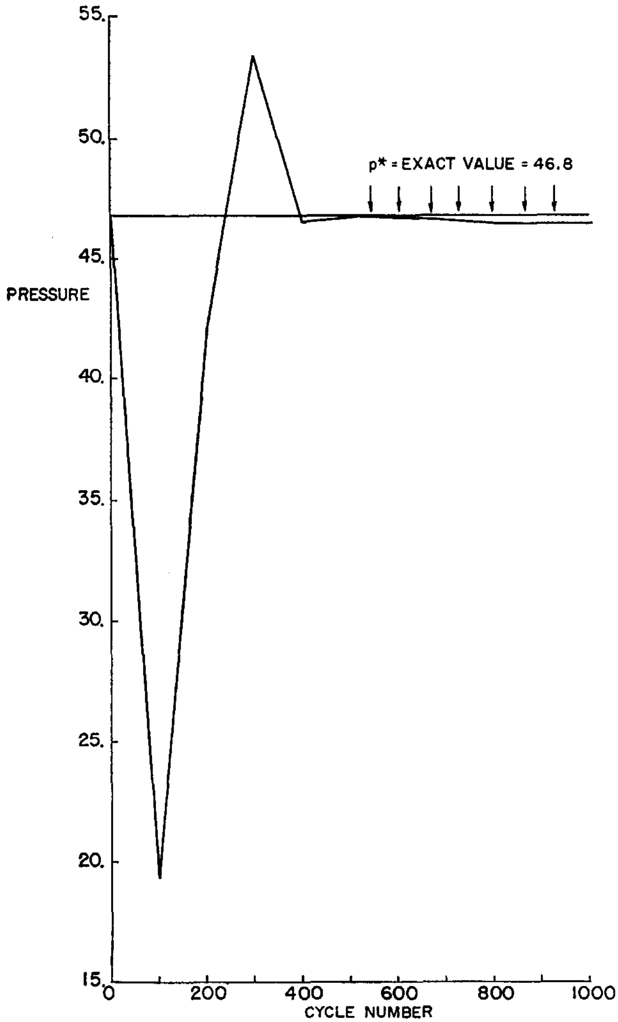

FIG. 7. Pressure at stagnation point vs cycle number.

3. *Standoff Distance of the Shock as a Function of Time*

The equations of motion assume that the gas appearing in the computation is a "gamma law" gas, that is, that

$$p = A\rho^{\gamma},$$

where A is a function of entropy S alone. Specifically [1, p. 10],

$$A = ke^{gS} \ (= 1 \text{ upstream}),$$

where k and g are positive constants. Thus A is a monotonic increasing function of S and can be used as a measure of the entropy jump across the shock. A simple method for determining the position of the shock would be to march from in front of the shock (the constant region) along a horizontal line until a point is reached at which A is greater than 1 and to assign the position of the shock to that point. Unfortunately, due to oscillation of the flow quantities, the quantity A oscillates below 1, then above; then sometimes the cycle repeats. Because of these irregularities, the position of the shock is taken to be halfway between the last point of an unbroken sequence of points at which $A = 1$ and the first point of an unbroken sequence of points with $A > 1$. The position of the shock on the line of symmetry is graphed in Fig. 8 according to this method, along with its theoretical

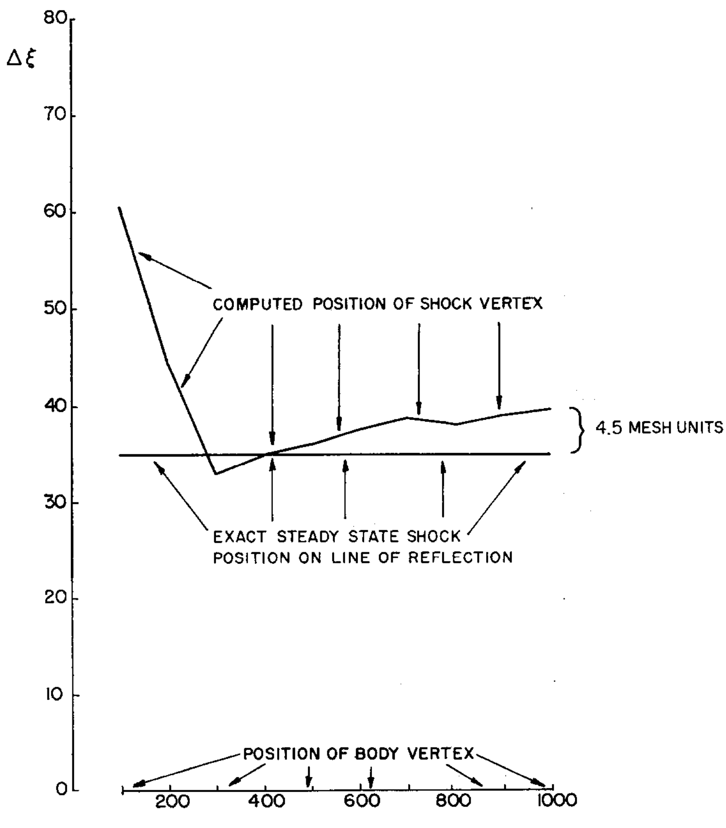

FIG. 8. Position of vertex of shock vs cycle number.

position in units of mesh points from the body. The position of the shock starts at 60.5, then it moves lower, and finally returns to a position around 39.5. The true position is 35 in these units. The body is at 0.

4. *Pressure Profile on the Body*

In Fig. 9, the pressure profile along the body is illustrated at three different times and the pressure curve obtained by interpolation from [4] is plotted on the same graph. As can be seen there, the pressure profile on the body at 100 cycles moves far below its exact position, then at 300 cycles far above, and then comes much closer to theoretical results at 1000 cycles. The pressure near the nose of the body (lower point number) is relatively more accurate than it is downstream.

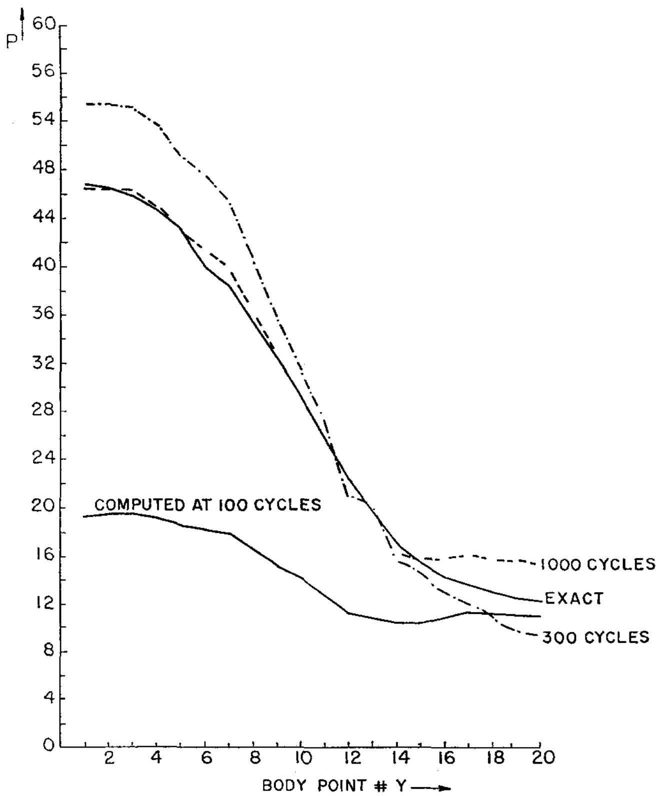

FIG. 9. Pressure vs Y along body. (– · –) Computed at 300 cycles; (——) exact; (– – –) computed at 1000 cycles.

5. *Final Shape of the Shock*

In Fig. 10, the position of the shock at 1000 cycles is illustrated and compared with its exact position and the position of the shock obtained by using a finite difference analogue of Eq. (29). It is clear that the conservation analogue gives much better results than Eq. (29), especially near the upper boundary.

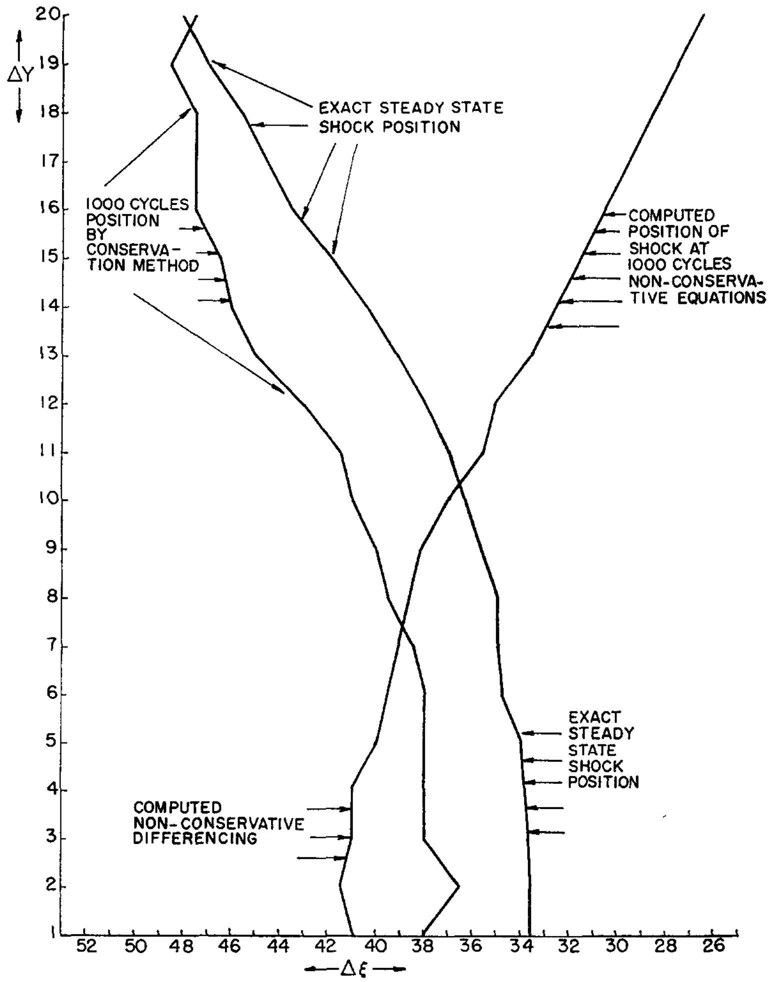

FIG. 10. Position of shock at 1000 cycles.

Acknowledgment

The author wishes to express his appreciation to Professor Peter D. Lax for numerous helpful suggestions; to Professor Robert D. Richtmyer for an introduction to the challenging scientific area of fluid dynamics computations; and to Professor Max Goldstein for his cooperation in using the computing center at the Courant Institute of Mathematical Sciences. Thanks are also due to Professor Samuel Burstein for a few short and stimulating discussions, and to Professor Eva Swenson for graciously communicating the results of her own investigations into detached shock calculations.

References

1. R. Courant and K. O. Friedrichs, "Supersonic Flow and Shock Waves," pp. 10 and 300. Interscience, New York (1948).
2. R. D. Richtmyer, "A Survey of Difference Methods for Non-Steady Gas Dynamics," National Center for Atmospheric Research Technical Note 63–2 (1963).
3. P. D. Lax and B. Wendroff, *Commun. Pure Appl. Math.* **13**, 217 (1960).
4. E. V. Swenson, "Numerical Computation of Hypersonic Flow Past a Two-Dimensional Blunt Body," AEC Research and Development Report NYO-1480-1. Courant Institute Mathematical Sciences, New York University, New York (1964).
5. S. Z. Burstein, "Finite Difference Calculations for Hydrodynamic Flows Containing Discontinuities." *J. Computational Phys.* **1**, 198 (1966).
6. J. von Neumann and R. D. Richtmyer, *J. Appl. Phys.* **21**, 232 (1950).
7. P. R. Garabedian and H. M. Lieberstein, *J. Aeronaut. Sci.* **25**, 109 (1958).
8. K. A. Bagrinovskii and S. K. Godunov, *Dokl. Akad. Nauk SSSR* **115**, 431 (1957).
9. D. Houghton, A. Kasahara, and W. Washington, *Monthly Weather Rev.* **94**, 141 (1966).
10. V. V. Rusanov, "The Calculation of the Interaction of Non-Stationary Shock Waves and Obstacles," *USSR Computational Math. and Math. Phys.* No. 2 (1962).
11. A. E. Taylor, "Advanced Calculus," p. 462. Ginn and Co., New York (1955).